FLEXIBLE JOINT CONTROL : ROBUSTNESS ANALYSIS OF THE COLLOCATED AND NON-COLLOCATED FEEDBACKS

D. Alazard — J.P. Chrétien

CERT-ONERA/DERA
2, Avenue E. Belin
TOULOUSE
France
Tel. (33) 61.55.70.16 — Fax. (33) 61.55.71.94
e-mail alazard@saturne.cert.fr

Paper presented at IROS'93
Intelligent Robots and Systems 93
Conference Center
Pacific Convention Plaza
Yokohama, Japan
Space Robotics and Control Session

FLEXIBLE JOINT CONTROL : ROBUSTNESS ANALYSIS OF THE COLLOCATED AND NON-COLLOCATED FEEDBACKS

D. Alazard — J.P. Chrétien
CERT-ONERA/DERA
2, Avenue E. Belin, TOULOUSE, France

Abstract: *In this paper, we propose a discussion on the robustness and performance properties of a proportional-derivative controller applied to a very flexible joint. Because of the flexible mode due to in-joint compliance, the classical collocated control does not allow to obtain good rigid mode dynamics with a correct phase margin in low and high frequency, and the non-collocated control does not allow to damp correctly the rotor mode. The simultaneous analysis of discrete root loci and Nichols plots leads to a phase control law with a derivative term built from both input and output velocities. Simulations taking into account various real non-linearities and measurement imperfections are proposed to validate this improved control design.*

Keywords: SPACE MANIPULATORS — JOINT — COLLOCATED CONTROL — P.D. CONTROL — ROTOR MODE

Introduction

Space manipulators have several specific features which limit the transfer of the terrestrial robotic know-how to the external space robots at any authority control level (cf.[1]) . From the point of view of joint control, the main difference comes from the rotor mode, due to in-joint compliance, which limits the performances achievable by position servo-loops. This problem is also considered for industrial robots, but the classical proportional-derivative controller built on the input velocity and the output position is often sufficient to insure the desired dynamics for the rigid mode without stability problems due to higher frequency dynamics : then, the collocation between the rate detector and the command torque guarantees a positive and active dissipation of the in-joint flexible modes. The robustness of this command is well-known and most of moto-reductors are provided with a tachometer on the input axis, mechanically tuned to the rotor, and a position encoder on the output axis.

For space manipulator joints, the rotor mode control problem becomes more significant due to the following considerations:

- beams of the arm are very long because of the great desired work-space : so, even in the case where the arm bears no payload, the total inertia (noted I_c) seen by each joint is very large ;
- as a counterpart and due to 0g environment, the motorization is very light. The solution which is often chosen to minimize the joint weight introduces a gearbox. But, the rotor inertia (noted I_r), even seen from the output axis through the square of the gear ratio, is very low and the succession of gear stages required to achieve an important reduction ratio yields to a very low stiffness (noted k).

On the collocated transfer function (fig.1), these conditions exhibit the fact that the residue of the flexible mode (equal to the inertia ratio I_c/I_r) is very important, and so, the limitation due to the cantilever pulsation, in terms of closed loop bandwidth, is very low [1]. But for very high ratios, even if this limit not attained in the course of space robotics activities, which allow slow motions because of the absence of productivity requirements, the classical P.D. controller loses its robustness property when the control law is discretized. This will be the subject of the first section of this paper. The numerical application is based on a real joint of a space robotic test facility called M.F.B. (Maquette Fonctionnelle de Bras manipulateur), developed by Matra Marconi Space under C.N.E.S. contract.

The second section is devoted to non-collocated control and shows how the frequency decoupling between the free mode and the cantilever mode permits to create easily a stabilizing but limited dissipation of the rotor mode with non-collocated P.D. control. This control built with both position and velocity on the output axis, basically unstable, presents a correct phase margin, once enhanced by a low-pass filter.

In the third section, a phase control making use of favorable properties of both collocated and non-collocated control is proposed. This new discrete time control design allows to reach the limit for the rigid dynamics fixed by the cantilever pulsation, but provides also a very good damping of the rotor mode and a correct phase margin.

In the last section, these previous analyses are validated with simulations taking into account non-linearities and measurement imperfections, and also the delay which appears in practice between the date of the measurement acquisition and the date of the command torque application to the joint.

1 Collocated control

The open loop model is shown on figure 1.

This work has been performed in the frame of contracts granted by C.N.E.S. — Centre Spatial de Toulouse (France) — under the technical management of M. Maurette.

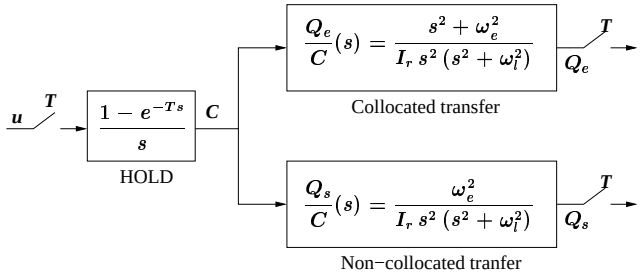

Figure 1 Open loop model

Notations and numerical application:

I_r	: rotor inertia ($1.3kg.m^2$)
I_c	: payload inertia ($53kg.m^2$)
$I = I_r + I_c$	: total inertia ($54.3kg.m^2$)
k	: joint stiffness ($17200Nm./rd$)
$\omega_e = \sqrt{\frac{k}{I_c}}$	: cantilever pulsation ($18.rd/s$)
$\omega_l = \sqrt{\frac{k(I_r+I_c)}{I_r I_c}}$	: free pulsation ($116.5rd/s$)
T	: sample period ($0.005s$)
Q_e	: input position (rd/s)
Q_s	: output position (rd/s)
C	: input torque (N.m)
u	: command (N.m)

Then, the collocated control feedbacks the input rate through a derivative gain K_v and the output position thought a proportional gain K_p and reads :

$$C = K_p.(Q_r - Q_s) - K_v.\dot{Q}_e$$

where Q_r represents the input reference position.

1.1 Continuous time tuning

As a first step, it is interesting to find the fastest closed loop dynamics for the rigid modes which are achievable by this control and the corresponding tuning with respect to the pulsation ratio ω_e/ω_l. That can be easily done using the following reduced parametrization (involving only dimensionless parameters) :

$x = \frac{\omega_e}{\omega_l}$	reduced cantilever pulsation
$\bar{s} = \frac{s}{\omega_l}$	reduced Laplace variable
$k_r = \frac{K_p}{I.\omega_l^2}$	reduced proportional gain
$\omega_r \ ; \ \frac{K_v}{I.\omega_l} = \frac{k_r}{\omega_r}$	reduced control dynamics

Table 1 Definition of reduced parameters

Then the closed loop transfer reads :

$$\frac{Q_s}{Q_r}(s) = \frac{K_p}{I.s^2.\left(1 + \frac{s^2}{\omega_l^2}\right) + K_v.s.\left(1 + \frac{s^2}{\omega_e^2}\right) + K_p}$$

or, with new parameters:

$$\frac{Q_s}{Q_r}(\bar{s}) = \frac{k_r}{\bar{s}^2.(1+\bar{s}^2) + \left[\frac{\bar{s}}{\omega_r}.\left(1 + \frac{\bar{s}^2}{x^2}\right) + 1\right]k_r}$$

For each value of parameter x, the closed loop eigenvalues yielding the fastest rigid dynamics is given by a root locus scaled according to k_r and optimal with respect to ω_r. The behavior of this optimal root locus is quite different for low values and for high values of parameter x. The boundary value between these two situations is given by $x_l = \frac{1}{\sqrt{6}}$. For this particular value, the optimal roots locus reveals a coalescent point on the real axis between five branches (see figure 2).

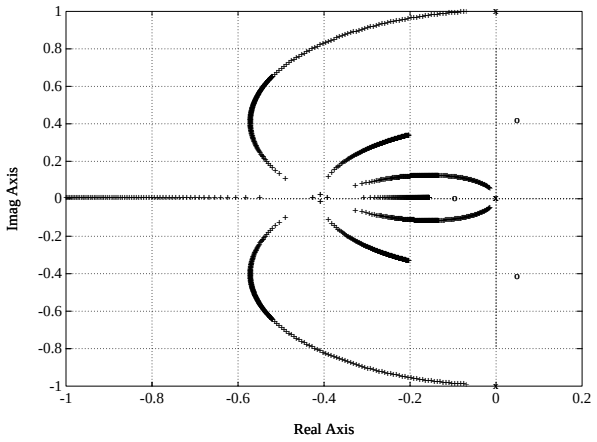

Figure 2 Optimal root locus with collocated P.D. controller ($x = \sqrt{\frac{1}{6}}$)

For higher values, (see figure 3) there is always a tuning (k_r, ω_r) for which the rigid poles are not attracted by the cantilever zeros and so, the limit for the closed loop rigid dynamics is given by the rotor mode stability which strongly depends on the natural damping (neglected in this analysis). This is typically the case of industrial robots and this case will not be investigated any longer in the sequel.

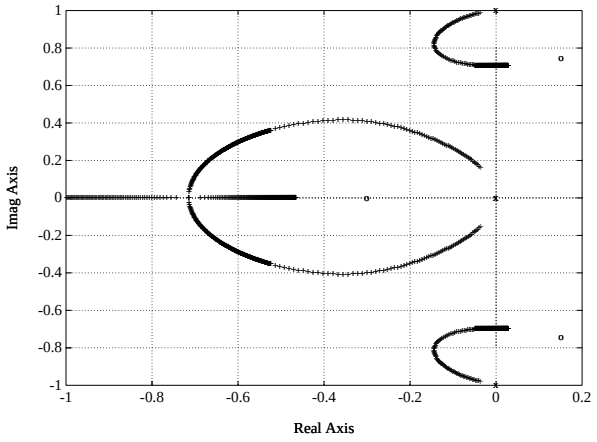

Figure 3 Optimal root locus with collocated P.D. controller ($x = 0.7$)

For values lower than x_l (see figure 4), the rigid poles are attracted by the cantilever zeros for any tuning (k_r, ω_r) while flexible poles are driven on the real axis. In this case, a good tuning is given by the couple (k_r, ω_r) which leads to 4 real eigenvalues:

- 3 equal eigenvalues corresponding to the two rigid poles and one of the two flexible poles ;
- 1 eigenvalue faster than the others due to the second flexible pole.

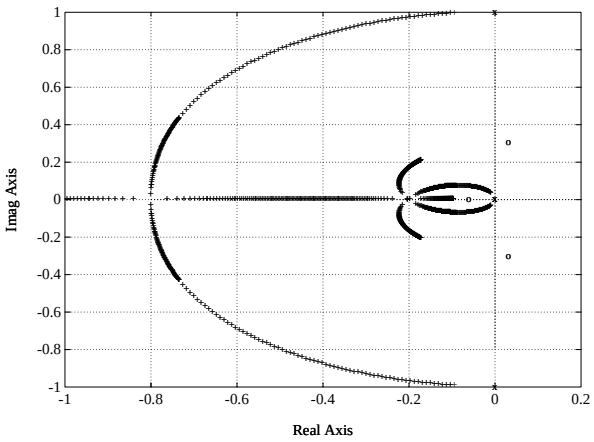

Figure 4 Optimal root locus with collocated P.D. controller ($x = 0.3$)

The following figure gives, for any value of x between $0.$ and $\frac{1}{\sqrt{6}}$:

- the common real eigenvalue λ_{opt} which specifies the rigid closed loop dynamics ;
- the corresponding optimal tuning k_r, ω_r; physical gains values (K_p, K_v) can be easily found with the help of table 1.

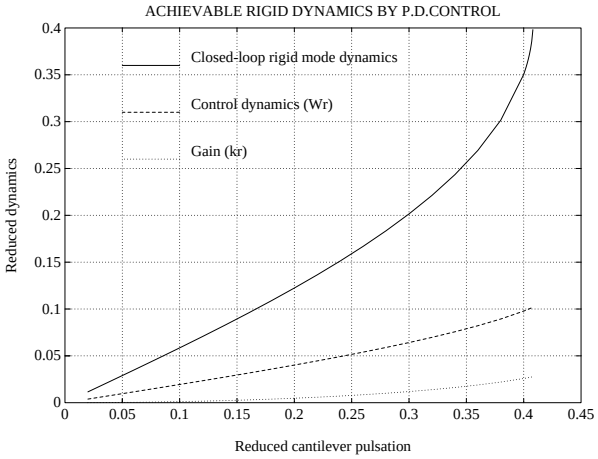

Figure 5 Optimal tuning for P.D. control

N.A. : In our case, this tuning gives the following result :

- $x = 0.15$;
- $K_p = 2030 \ N.m/rd$;
- $K_v = 575 \ N.m.s/rd$;
- Dynamics : $\{-10.7; -10.7; -10.7; -436.9\}$;

1.2 Discrete time tuning

It is quite obvious that the sampling of the previous control law gets into trouble with the fast pole ($-437 rd/s$) : Fig. 6) shows that the real negative asymptote goes outside the unit circle in the z plane.

If we want to keep the same control architecture, two solutions are possible:

- reduce the rigid mode dynamics until the fast pole comes back inside the unit circle;
- in order to keep the optimal rigid dynamics, introduce a first order low-pass filter in the loop [1].

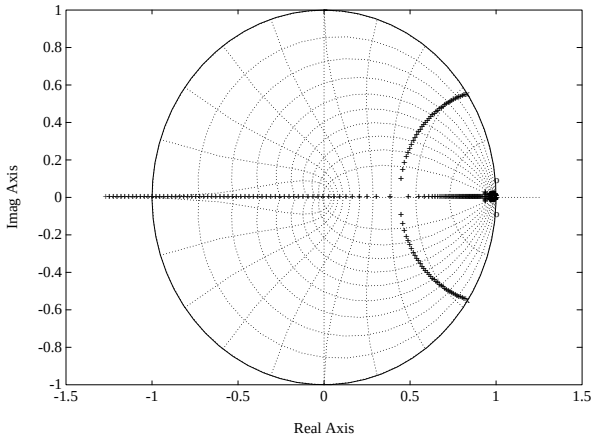

Figure 6 Nominal discrete root locus with collocated control

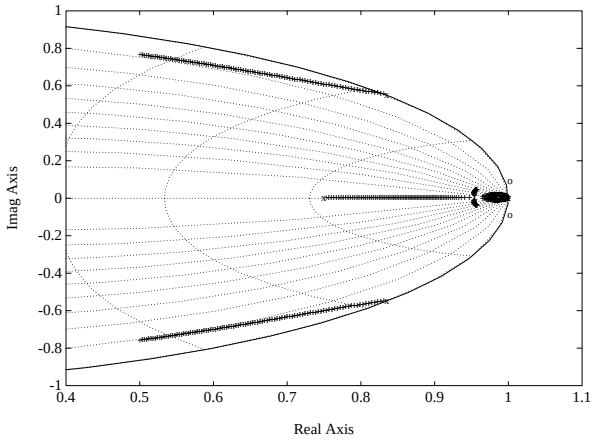

Figure 7 Discrete root locus with filtered collocated control

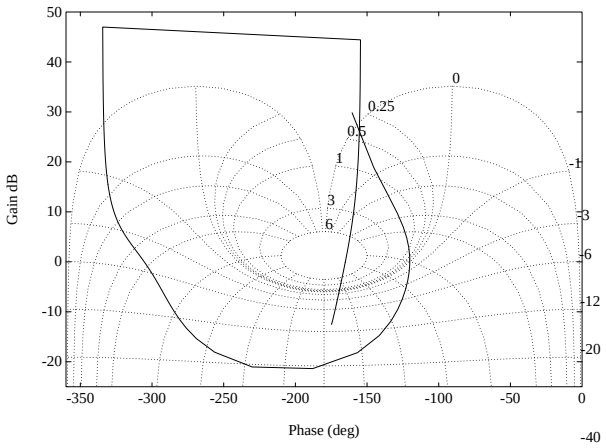

Figure 8 Discrete Nichols plot with filtered collocated control

The root locus of this last solution with a $50. rd/s$ filter cut-off frequency is displayed on figure 7. The dynamics of the rigid mode are correct, the rotor mode is stabilized, but the discrete Nichols plot analysis reveals an insufficient phase margin (see figure 8) : the rigid mode phase margin is large ($70°$), but the phase margin over $120 rd/s$ is quite small ($15°$) and easy to loose with actuators or detectors dynamics or delay in control calculation. So, in the case of very high inertia or pulsation ratios, the classical collocated control does not allow to obtain simultaneously good rigid dynamics bandpass and a correct phase margin in high frequency.

2 Non-collocated control

The command reads now :

$$u = K_p.(Q_r - Q_s) - K_v.\dot{Q}_s \ ,$$

and naturally yields a rotor instability according to the following Nichols plot :

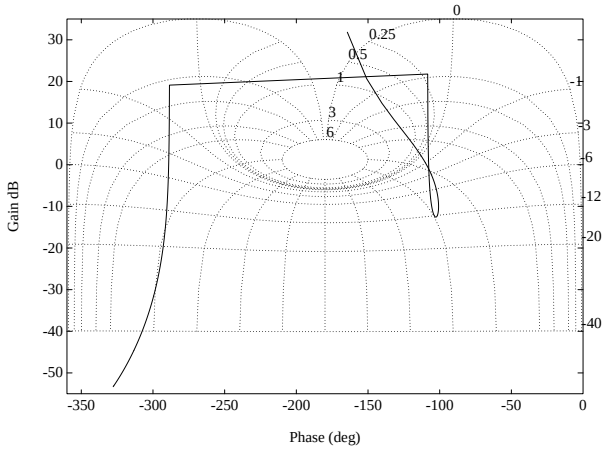

Figure 9 Discrete Nichols plot of non-collocated P.D. control

But we can also see on this locus that stability can be restored with a phase shift which minimal value must be at least equal to $90°$ at the rotor mode frequency. That can be easily done with a second order low-pass filter, for instance :

$$u_1 = K_p.(Q_r - Q_s) - K_v.\dot{Q}_s \ ; u = u1.\left(\frac{50.T.z}{z - 1 + 50.T}\right)^2$$

The corresponding Nichols plot (with previous gains K_p and K_v) is displayed on figure 10. The margin in high frequency becomes now equal to $150°$ and the root locus (figure 11) shows clearly that the artificial dissipation function of the rate feedback is restored at the free mode frequency.

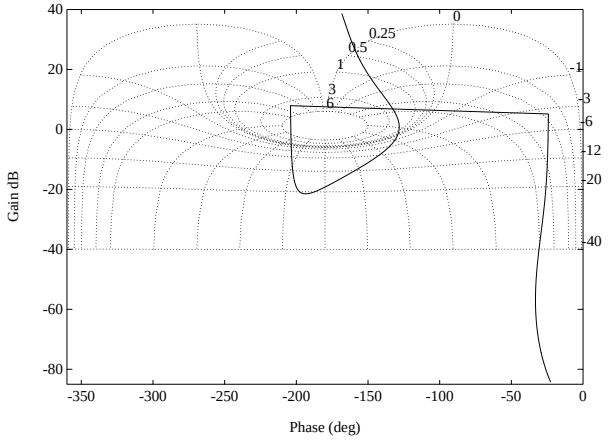

Figure 10 Discrete Nichols plot of filtered non-collocated control

The frequency decoupling between the rigid mode and the rotor mode ensures that the filter does not alter the rigid mode branch on the root locus, and then that the rigid dynamics performances are preserved. The only drawback of this control design is that the achievable damping of the rotor mode is not large enough.

It is easy to show also that a pure delay has a similar stabilizing effect. The main feature of a pure delay is a phase

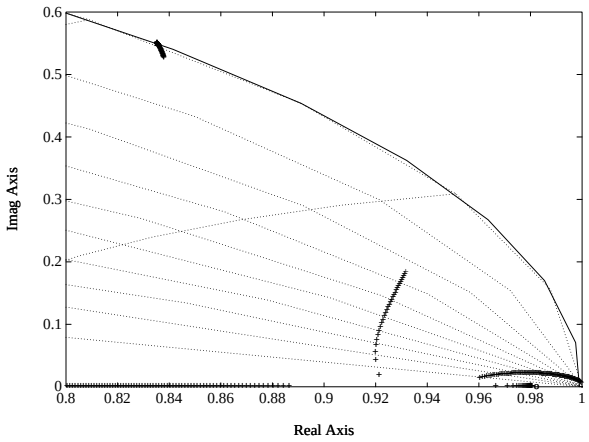

Figure 11 Discrete root locus of filtered non-collocated control

which is a linear function of the pulsation without any gain attenuation. The number N of sample periods required for a phase shift ϕ (in radians) at the rotor pulsation ω_l is given by :

$$N.T.\omega_l = \phi$$

For instance, with $\phi = 180°$, an equivalent control law reads :

$$u_1 = K_p.(Q_r - Q_s) - K_v.\dot{Q}_s \ ; u = u1.z^{-5}$$

with the corresponding root locus displayed on figure 12

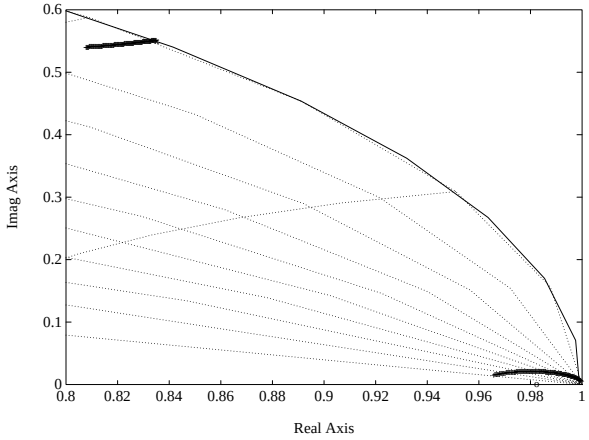

Figure 12 Root locus of delayed non-collocated P.D. control law

It changes the sign of the control at the rotor mode frequency, which is clearly what is needed to restore a correct sign relationship between the control and the rate measurement ; of course, the sign of the control in low frequency *must* remain that of a negative feedback.

3 Phase control

The previous investigations have shown that the collocated rate feedback which is required to damp correctly the rigid mode has too much influence on the rotor mode and thus produces a very fast pole which cannot stand the control sampling without major degradation of the phase margin at the free mode frequency.

On the other hand, the non-collocated control can be stabilized with a filter or a pure delay and then presents a good phase margin together with good dynamics for the rigid mode, but the rotor mode is not enough damped.

So, it is interesting to use both input and output rate feedbacks : each of these feedbacks must be phase controlled in order to create a positive dissipation at the rotor mode frequency. The final tuning that we propose reads:

$$u = -100\,\frac{z-1}{z-1+50.T}\,\frac{z-1}{z.T}Q_e \quad \text{(inner loop)}$$
$$+z^{-5}\left[2000(Q_r - Q_s) - 600\,\frac{z-1}{z.T}Q_s\right] \quad \text{(outer loop)}$$

Corresponding root loci are displayed on figure 14 for the inner loop (built on input rate measurement), and on figure 15 for the external loop (built on output position and rate measurements).

Figure 13 Final control design

As we can see, the rigid mode control is entirely done by the external loop. A pure delay is introduced to provide the phase shift required to create active damping from the output rate. This loop is completed by an inner loop built on input rate to increase the damping of rotor mode. This last loop is high-pass filtered in order to :

- attenuate the influence of this loop on the rigid mode (controlled by external loop) ;
- bring the correct phase shift at the rotor mode pulsation.

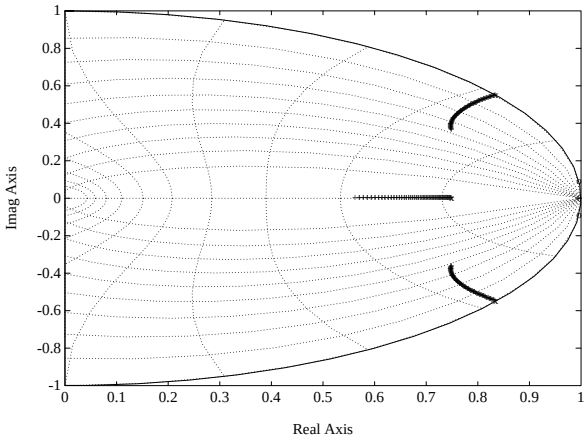

Figure 14 Root locus of input rate feedback

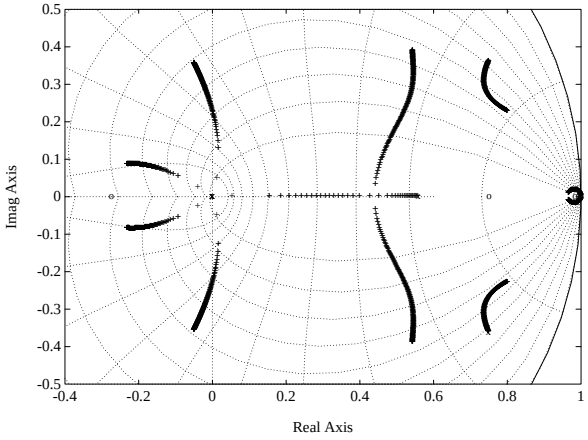

Figure 15 Root locus of external loop

Final closed loop dynamics (and continuous time equivalents) are displayed in the following table :

Discrete time dynamics	Continuous time equivalent	nature
0.9661 + 0.0088i	6.9 + 0.018i	rigid mode
0.8012 + 0.2275i	36. + 55.i	flexible mode
0.5427 + 0.3907i	80. + 125.i	control mode
-0.0501 + 0.3569i	204. +342.i	control mode
-0.2315 + 0.0855i	280. + 558.i	control mode

Table 2 Final closed loop dynamics

The minimum damping is over 0.5 and the rigid dynamics are good enough. From the robustness point of view, the Nichols plot (figure 16) reveals correct phase and gain margins at any frequency and seems to be alike the one which can be obtained with P.D. control on a rigid joint.

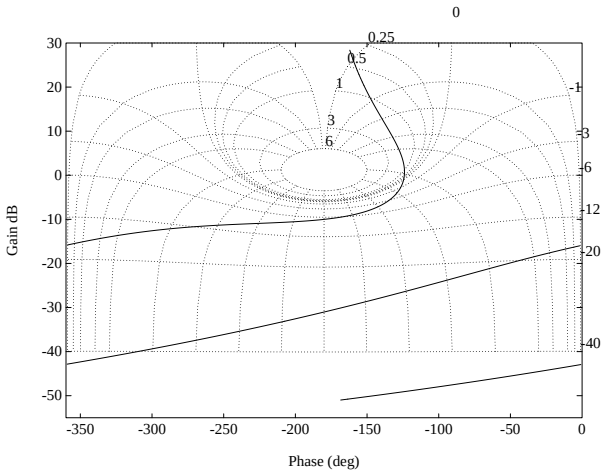

Figure 16 Nichols plot of external loop

4 Simulations results

From the implementation point of view, several constraints appear and limit the results obtained in previous theoretical analyses. A second step before real implementation thus consists in a validation with a simulation tool taking into account various non-linearities and measurement imperfections. Among all these constraints, the most important one is the measurement quantization because we have seen that the rigid mode was entirely controlled by output rate and position, the measurement of which is available on the mock-up joints through optical position encoders only. So, we can notice on the final control scheme (figure 13) that velocities are simply derived from position measurements by Euler formula : it is easy to check, on root loci and Nichols plots, that these finite differences do not alter too much the previous results (assuming the rate measurements available). But we have to prove that the output resolution (here $65000\ pt/revs$) is adequate to control the rigid mode. This last problem is not so important with classical control using rotor axis measurements because the resolution is then the input one times the reduction ratio (here $18000\ pt/revs * 100$). The simulations presented figure 17 for the collocated and filtered control, and figure 18 for the

final design take into account these quantizations, and also :

- the input torque saturation
- dry and viscous friction

We have investigated a variation of the value of the pure delay introduced in the loop to take into account:

- the control law computation time (typically $0.001s$),
- the electrical mode (PWD) which can be modeled by a first order filter with a 0.002s response time.

The collocated control is not robust to the pure delay and becomes unstable, as a consequence of the small phase margin of this design. Time responses obtained with phase control are insensitive to this delay and the desired behavior is not affected by the measurement quantization.

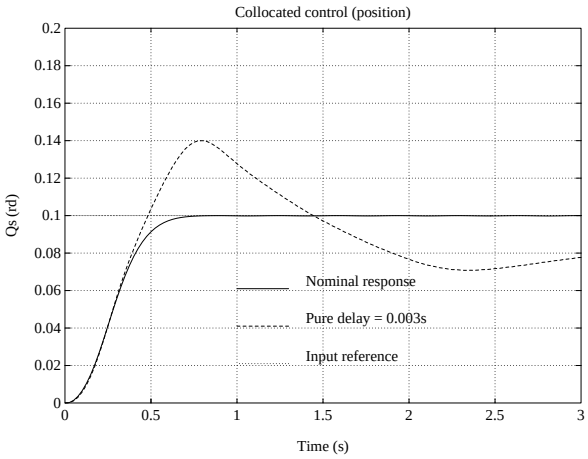

Fig 17 Collocated filtered P.D. control

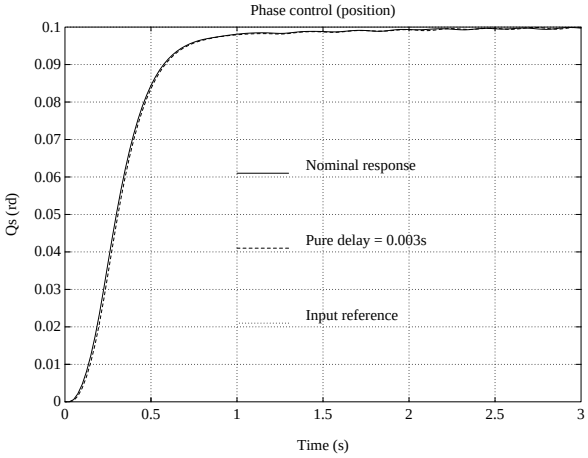

Figure 18 Phase control

5 Conclusions

Space dimensioning of the M.F.B. mock-up have led us to stress some specific problems from the joint control point of view. The in-joint flexible mode becomes a major dynamic parameter for the control law synthesis and can drive classical rotor axis collocated control to instability. In order to achieve rigid mode performance, we have investigated improvements of the basic proportional-derivative control laws, which appear more suitable for joint low authority control requiring good robustness properties with respect to arm and payload configurations than complex solution involving pole/zeros cancellation or very high order controller. The final proposed solution is a simple phase control, using both rotor axis and output axis measurements, ensuring the closed-loop bandwidth achievable by P.D. control with better phase margin and rotor mode damping. The next step of the studies will be the implementation of this control design on the various M.F.B. joints.

References

[1] D. Alazard, J. P. Chrétien, T. Blais, and J. P. Hermier, "MFB : design, implementation and test of improved joint control for space service manipulators," in *i-SAIRAS, International Symposium on Artificial Intelligence, Robotics and Automation in Space*, (Toulouse-Labège, France), Sept. 30th - Oct. 2nd 1992.

[2] J. P. Hermier, T. Blais, V. Germain, and E. D'Andrimont, "M.F.B. 5," rapport final, M.M.S, Septembre 1991.

[3] R. J. Gorter, A. V. Swieten, A. Veltman, and P. P. J. V. den Bosch, "Modelling and control of a HERA joint," in *IFAC, Automatic Control in Aerospace (preprints)*, (München), pp. 371–376, September 1992.

[4] D. Alazard and J. P. Chrétien, "Modélisation, simulation et commande d'une articulation de bras manipulateur," Rapport Final 2/7789a(texte), b(planches), CNES/DERA, Janvier 1992.

[5] J. P. Chrétien, "Digital attitude control design for space applications," *ESA Journal*, vol. 5, no. 1, pp. 229–241, 1981.

[6] J. P. Chrétien, P. Rodrigo, M. Gauvrit, D. Bontoux, and J. Jodeau, "Preliminary study of digital attitude control design techniques for satellite," Technical Report 1/7171, ESTEC/DERA, 1979.